https://doi.org/10.5194/egusphere-2026-2969
Preprint. Discussion started: 7 September 2026

Reducing parameter uncertainty in the Noah-MP-Crop model through global sensitivity analysis and targeted optimization

Zhonghe Li[a,b†], Le Chen[c†], Chesheng Zhan*[b,e], Shi Hu[d], Like Ning[f], Lanfang Wu[b], Hai Guo[b], Qi Zhang[g]

[a] *Central South Academy of Inventory and Planning of NFGA, Changsha 410014, Hunan, China*

[b] *Key Laboratory of Ecosystem Network Observation and Modeling, Institute of Geographic Sciences and Natural Resources Research, Chinese Academy of Sciences, Beijing 100101, China*

[c] *College of the Environment and Ecology, Hunan Agricultural University, Changsha, Hunan 410128, China*

[d] *Key Laboratory of Water Cycle and Related Land Surface Processes, Institute of Geographic Sciences and Natural Resources Research, Chinese Academy of Sciences, Beijing 100101, China*

[e] *Yucheng Comprehensive Experiment Station, Chinese Academy of Science, Beijing 100101, China*

[f] *Ministry of Education Key Laboratory for Earth System Modeling, Department of Earth System Science, Tsinghua University, Beijing, 100084, China*

https://doi.org/10.5194/egusphere-2026-2969
Preprint. Discussion started: 7 September 2026

[g] *Space Engineering University, Beijing 101416, China*

† **These authors contributed equally to this work.**

Corresponding Author: Chesheng Zhan

E-mail: zhancs@igsnrr.ac.cn

https://doi.org/10.5194/egusphere-2026-2969
Preprint. Discussion started: 7 September 2026

Reducing parameter uncertainty in the Noah-MP-Crop model through global sensitivity analysis and targeted optimization

Abstract : Accurately representing crop growth in land surface models (LSMs) is crucial for capturing cropland – atmosphere interactions, but in practice this remains challenging because many crop-related parameters are poorly constrained. In this study, we focus on reducing parameter uncertainty in the Noah-MP-Crop model by combining global sensitivity analysis with a targeted parameter optimization approach. We first assess the sensitivity of simulated crop yield and leaf area index (LAI) using the Morris screening method and Sobol' variance decomposition at nine agricultural experimental sites across China. Across sites and crops, the analysis consistently points to parameters associated with CO_2 assimilation and carbon use efficiency as the primary controls on crop growth simulations. In contrast, parameters describing crop structure and phenology tend to matter most at specific growth stages rather than throughout the entire season. Guided by these sensitivity results, we then apply a targeted optimization strategy, in which the ranges of key parameters are progressively refined using an interval-based search framework. Comparison with field observations shows clear improvements after optimization: yield RMSE is reduced by 25-86%, LAI-related objective function values decrease by 49-90%, and mean absolute errors drop by 40-80% across major crop types. Overall, our results suggest that sensitivity-guided parameter optimization provides a practical and efficient way to reduce parameter uncertainty in Noah-MP-Crop. The optimized model better reproduces observed LAI and yield dynamics across different climatic regions, offering useful insights for improving crop representation in land surface models.

Key words: Noah-MP-Crop; parameter uncertainty; sensitivity-guided optimization; global sensitivity analysis; crop yield and leaf area index

1 Introduction

Cropland constitutes a major component of terrestrial ecosystems and plays a key role in

https://doi.org/10.5194/egusphere-2026-2969
Preprint. Discussion started: 7 September 2026

regulating exchanges of water, energy, and heat between the land surface and the atmosphere (Levis et al., 2012). Through crop growth and agricultural management, both biophysical and biochemical surface processes are modified, leading to changes in land surface properties such as leaf area index (LAI) and albedo. These changes, in turn, affect atmospheric water vapor and temperature patterns at regional scales (Lobell et al., 2006; Pitman et al., 2009). As a result, accurately representing crop growth in land surface models (LSMs) has become increasingly important for understanding and quantifying cropland-atmosphere feedbacks.

Over the past few decades, coupling crop growth models with LSMs has emerged as a widely used framework for exploring how cropland dynamics influence land-atmosphere interactions across different spatial and temporal scales (Yu et al., 2022). Within this framework, the realism of simulated crop growth processes largely determines how well cropland ‐ atmosphere feedbacks can be captured. Early modeling efforts often relied on prescribed LAI values derived from lookup tables or monthly remote sensing products to represent crop phenology and productivity in a simplified manner (Rodell et al., 2004). While this approach is computationally efficient, it assumes relatively static vegetation conditions and therefore struggles to reflect the dynamic responses of crops to climate variability and agricultural management (Fang et al., 2001).

To overcome these limitations, recent generations of LSMs have increasingly incorporated explicit crop growth modules that simulate crop development and physiology in a process-based way. Well-known examples include SiB-Crop (Lokupitiya et al., 2009), JULES-SUCROS (Van den Hoof et al., 2011), CLM-Crop (Drewniak et al., 2013), and JULES-InfoCrop (Tsarouchi et al., 2014). Following this trend, the Noah land surface model with multiparameterization options (Noah-MP; Niu et al., 2011) has introduced a dynamic crop module that represents crop growth stages using cumulative growing degree days (GDD) (Liu et al., 2016). These developments mark an important step toward more realistic cropland simulations. However, despite the added process detail, crop growth simulations in LSMs remain subject to substantial uncertainty, largely due to the complexity of land surface processes and the large number of poorly constrained model parameters.

Several efforts have been made to reduce uncertainty within the Noah-MP-Crop framework. These include the implementation of an irrigation scheme (Xu et al., 2019), model evaluation and application over the U.S. Midwest (Zhang et al., 2020), and the assimilation of observational

https://doi.org/10.5194/egusphere-2026-2969
Preprint. Discussion started: 7 September 2026

datasets, such as LAI, soil moisture, and solar-induced chlorophyll fluorescence, using ensemble Kalman filter techniques (Xu et al., 2021). While these studies have improved model performance to some extent, parameter uncertainty remains a major source of error, particularly as newer versions of Noah-MP-Crop introduce an increasing number of crop-specific parameters to better describe diverse crop growth processes (Liu et al., 2016).

Inaccurate or poorly constrained parameter values are widely recognized as a key limitation in environmental modeling (Gupta et al., 1998), underscoring the need for effective parameter optimization strategies (Rosolem et al., 2013). Existing approaches to crop model parameter optimization can generally be divided into traditional and intelligent methods. Traditional approaches, such as sensitivity analysis, trial-and-error calibration, and systematic parameter searches, offer valuable insights into parameter effects, but they are often computationally expensive and sensitive to initial parameter settings (Pianosi et al., 2016). In contrast, intelligent optimization methods, including genetic algorithms (GA), particle swarm optimization (PSO), and simulated annealing, have been proposed as more flexible alternatives. These methods have been successfully applied in crop modeling studies, such as optimizing soybean parameters using GA (Boote et al., 2003), winter wheat parameters using PSO (Wagner et al., 2020), and maize growth in CERES-Maize using simulated annealing (Ferreyra et al., 2004).

Despite their demonstrated effectiveness, intelligent optimization methods can become difficult to apply when models involve high-dimensional parameter spaces and strong parameter interactions. Under such conditions, the computational burden increases rapidly and the risk of overfitting becomes non-negligible. Interval-based parameter search approaches provide a potentially more efficient alternative by narrowing parameter ranges and reducing the overall search space. These approaches have shown promising results in multi-objective optimization problems (Balderas et al., 2019) and in irrigation management under uncertainty using interval-based fuzzy programming techniques (Zhang et al., 2020). Together, these studies suggest that interval-based strategies can improve both the efficiency and robustness of parameter optimization in complex environmental models.

Parameter optimization alone, however, is rarely sufficient if it is not informed by an understanding of which parameters actually matter. Sensitivity analysis (SA) offers a systematic way to quantify parameter influence through repeated model simulations and has been widely

https://doi.org/10.5194/egusphere-2026-2969
Preprint. Discussion started: 7 September 2026

used to reduce parameter dimensionality and improve optimization efficiency (Pianosi et al., 2015; He et al., 2021). In crop modeling, SA has proven especially valuable for identifying key parameters controlling crop growth and yield, thereby simplifying calibration procedures and improving model performance (Confalonieri et al., 2010; Wang et al., 2013; Silvestro et al., 2017; Jin et al., 2018; Lu et al., 2021). Within the Noah-MP framework, sensitivity-based approaches have been applied to improve vegetation dynamics by optimizing soil and vegetation parameters (Niu et al., 2020; Sun et al., 2021; Shu et al., 2022). In contrast, the role of crop-specific parameters in controlling growth processes within the Noah-MP-Crop model has received comparatively little attention, limiting a systematic understanding of parameter importance in crop simulations. To address this gap, this study conducts a comprehensive sensitivity analysis of crop-related parameters in the Noah-MP-Crop model and links the results directly to a targeted parameter optimization strategy. By explicitly coupling sensitivity analysis with optimization, the proposed approach aims to reduce parameter uncertainty and improve the robustness of crop growth simulations under diverse environmental conditions.

Specifically, this study investigates the key parameters controlling crop growth processes in Noah-MP-Crop and evaluates how sensitivity-guided parameter optimization can improve crop growth simulations across China. Using observations of crop yield and leaf area index (LAI) from nine agricultural experimental sites, we first identify influential and non-influential parameters and quantify their relative contributions to output variability. We then refine the most influential parameters through targeted optimization and assess the resulting improvements in model performance. Through this analysis, the study seeks to reduce parameter uncertainty in Noah-MP-Crop and provide practical guidance for calibrating crop-related parameters in land surface models.

2. Materials and methods

This study uses the Noah-MP-Crop model as the core framework for simulating crop growth and develops a new parameter optimization strategy to improve model performance. Because the static crop-related input data required by Noah-MP-Crop have so far been validated only for the United States, and no ready-to-use dataset exists for simulating crop growth in China, it was first

https://doi.org/10.5194/egusphere-2026-2969
Preprint. Discussion started: 7 September 2026

necessary to construct crop-specific static input data suitable for Chinese conditions. This step provides the basic support needed to apply the Noah-MP-Crop model in this study.

On this basis, a sensitivity analysis was carried out to systematically identify the parameters that exert the strongest control on crop growth simulations. During the sensitivity analysis, a large number of random parameter combinations were generated, and these parameter sets were then reused within a newly developed optimization framework to refine the most influential parameters. In this way, parameter sensitivity and optimization were directly linked, allowing the optimization process to focus on parameters that matter most.

Model evaluation was based on observed crop yield and leaf area index (LAI) data collected from nine agricultural field stations distributed across different climatic regions in China. Although crop yield and LAI observations were available for the period 2004-2008, the LAI dataset for 2005 was the most complete. Therefore, only the 2005 yield and LAI observations were used for parameter optimization. After optimization, the model was further evaluated against multi-year observations from 2004 to 2008 to assess its overall performance and robustness.

2.1 Study area

In this study, the research area comprised nine agricultural experimental sites (Fig. 1). Two sites, Hailun (HL) and Shenyang (SY), were located in northeast China, characterized by mean yearly temperatures of 2.4℃ and 8.6℃, respectively, and average annual rainfall of 580mm and 712mm. Intercropping of spring maize and soybean took place during the growing season from April to October each year in these regions.

Three sites, Fengqiu (FQ), Yucheng (YC), and Luancheng (LC), were situated in north China. The average annual temperature in this region was approximately 14℃, with an average annual rainfall of around 600mm. The area featured a warm temperate subhumid continental monsoon climate. The primary crops grown in this region were summer maize and winter wheat. The growing season for summer maize spanned from June to September, while winter wheat was cultivated from October to June of the following year.

The remaining four sites, namely Yanting (YanT), Taoyuan (TY), Yingtan (YingT), and Changshu (CS), were located in the middle and lower reaches of the Yangtze River in China.

https://doi.org/10.5194/egusphere-2026-2969
Preprint. Discussion started: 7 September 2026

These areas had an average annual temperature exceeding 15℃ and annual precipitation surpassing 1000mm. Early-season rice and single cropping rice were cultivated during the growing season from March to May and April to July, respectively, in these regions.

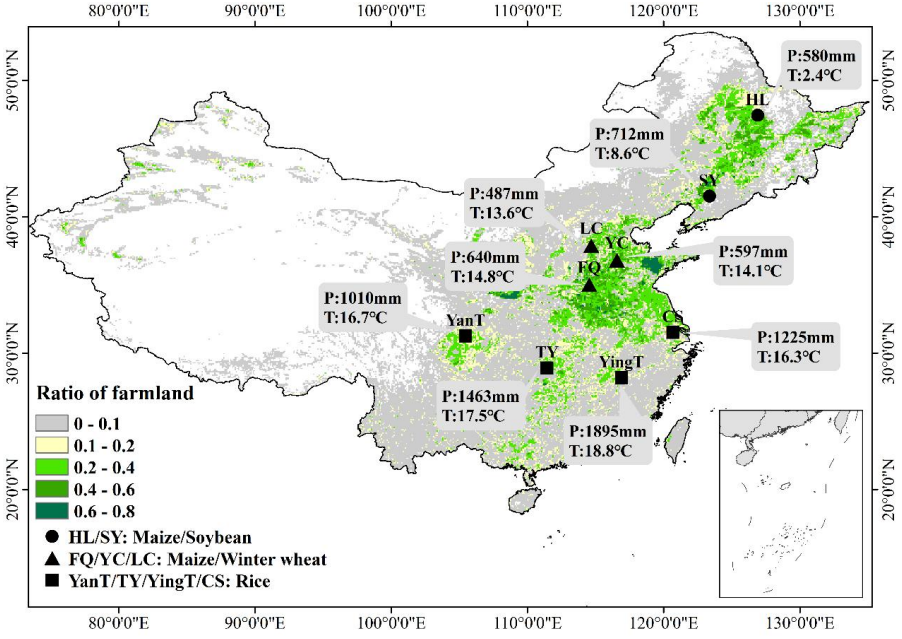

Fig.1 The spatial distributions of agricultural ecology experimental stations. The histograms represent the meteorological information of 9 agroecological experiment stations. P and T represent the precipitation and temperature, respectively. Meteorological data are multi-year average from 1980 to 2018 (Chinese Ecosystem Research Network Data Center, http://www.nesdc.org.cn/) (Wang et al., 2017).

2.2 Noah-MP-Crop model

The Noah-MP-Crop model extends Noah-MP by coupling canopy radiation, energy – water exchange, and process-based crop growth and carbon allocation modules to simulate crop development responses to environmental conditions (Liu et al., 2016; Niu and Yang, 2004; Zhang et al., 2020).

Photosynthesis in light and shade leaves is calculated separately, considering factors such as light restriction, carboxylase restriction (Rubisco), and export restriction (C3). The total photosynthesis rate (A) in units of g m^{-2} s^{-1} is calculated as follows (Niu et al., 2011),

$$A = 12 \times 10^{-6}(A_{\text{sun}} L_{\text{sun}} + A_{\text{shd}} L_{\text{shd}}) \quad (1)$$

https://doi.org/10.5194/egusphere-2026-2969
Preprint. Discussion started: 7 September 2026

where A_{sun} and A_{shd} represent the photosynthesis rates of light and shade leaves, respectively, and L_{sun} and L_{shd} denote the leaf area index (LAI) of light and shade leaves, respectively. The light restriction ($A_{l,i}$), carboxylase restriction (Rubisco, A_c) and export restriction (A_s) are represented by:

$$A_{L.i} = \frac{(c_i - c_{cp}) \times 4.6 \times QE \times PAR_i}{c_i + 2 \times c_{cp}} \quad (2)$$

$$A_c = \frac{(c_i - c_{cp}) \times VMAX}{c_i + K_c \times (1 + o_i / K_o)} \quad (3)$$

$$A_s = 0.5 \times VMAX \quad (4)$$

where c_i is the CO_2 concentration of leaf cavity, PAR_i is photosynthetically active radiation (W m^{-2}), c_{cp} is the CO_2 compensation point, K_c and K_o (pa) are the Michaelis- Menton constants for CO_2 and O_2, QE is the quantum efficiency and $VMAX$ is the maximum carboxylation rate, which is quantified as:

$$VMAX = VMAX25 \times a_{VMAX}^{\frac{T_v - 25}{10}} \times F(N) \times F(T_v) \times \beta \quad (5)$$

where $VMAX25$ is the maximum carboxylationrate at 25℃, a_{VMAX} is a temperature sensitive parameter, $F(N)$ a function that mimics thermal breakdown of metabolic processes, $F(T_v)$ is a foliage nitrogen factor, and β is the soil moisture controlling factor. Carbohydrates produced by photosynthesis are represented as:

$$CBHYDRAFX = A \times 30 \times IPA \times (1 - \beta) \times uca \quad (6)$$

where IPA is the planting index of crop (1 or 0) and uca is a conversion factor ($uca = 10^{-6}$).

In the Noah-MP-Crop model, crop phenological development is controlled by accumulated growing degree days (GDD), which are used to delineate different growth periods throughout the cropping cycle (Liu et al., 2016). The full growth cycle is divided into eight phenological growth stages (PGS1-PGS8), spanning from the pre-planting phase to post-harvest conditions. Crop growth dynamics in the model are tightly linked to the evolution of leaf area index (LAI), which serves as a key state variable connecting biomass accumulation and photosynthetic activity.

LAI is updated on a daily basis according to simulated leaf biomass and crop-specific specific leaf area (BIO2LAI). The updated LAI is then used as an input for calculating photosynthesis on subsequent days, forming a feedback between growth and carbon assimilation:

$$LAI = Leaf_{mass} \times BIO2LAI \quad (7)$$

where $Leaf_{mass}$ represents crop leaf biomass, $BIO2LAI$ denotes the specific leaf area.

https://doi.org/10.5194/egusphere-2026-2969
Preprint. Discussion started: 7 September 2026

Carbon assimilated through photosynthesis is distributed among different plant carbon pools according to allocation fractions that vary by growth stage, with values ranging between 0 and 1. During this process, part of the assimilated carbon is consumed by leaf respiration, which includes both maintenance respiration and growth respiration. The maintenance respiration of leaves (RSLEAF) is calculated as follows:

$$RSLEAF = LFMR25 \times TF \times FNF \times LAI \times (1-\beta) \times 30 \times uca \quad (8)$$

where LFMR25 is the leaf maintenance respiration rate at 25℃, *TF* is a temperature-dependent factor, *FNF* is a nitrogen regulation factor for respiration and, *uca* is a unit conversion factor (*uca* = 10^{-6}).

Leaf growth respiration (*GRLEAF*) is then determined as a fixed fraction of the remaining carbon after accounting for maintenance respiration:

$$GRLEAF = FRA\_GR \times (LFPT(PGS) \times CBHYDRAFX - RSLEAF) \quad (9)$$

where *FRA_GR* denotes the fraction allocated to growth respiration, *LFPT(PGS)* represents the fraction of carbohydrates allocated to leaves at a given growth stage,and CBHYDRAFX is the total carbon available for allocation.

2.3 Data

2.3.1 Forcing data

Atmospheric forcing data used in this study were obtained from the Global Land Data Assimilation System (GLDAS; https://ldas.gsfc.nasa.gov/gldas/), a global land surface dataset jointly developed by the National Aeronautics and Space Administration (NASA) Goddard Space Flight Center (GSFC) and the National Oceanic and Atmospheric Administration (NOAA) National Centers for Environmental Prediction (NCEP). GLDAS is designed to provide spatially and temporally consistent land surface forcing fields for land surface and hydrological modeling applications.

The GLDAS dataset provides global coverage from 1948 to 2020, with spatial resolutions of 0.25°×0.25° and 1°×1°, and temporal resolutions ranging from 3-hourly to monthly. In this study, we used the GLDAS_NOAH2.1 product, which offers a 0.25° × 0.25° spatial resolution and a

https://doi.org/10.5194/egusphere-2026-2969
Preprint. Discussion started: 7 September 2026

3-hourly temporal resolution, making it suitable for driving the Noah-MP-Crop model.

Meteorological forcing data covering the period 2000-2008 were used to drive the model simulations. Among these, data from 2005 were selected for parameter optimization, while the full multi-year period was retained for subsequent model evaluation.

2.3.2 Statical data

The static input data related to crops mainly include crop type, planting date, harvest date, and irrigation ratio. Crop type and irrigation ratio were derived from the SPAM2010 (Spatial Production Allocation Model) dataset, which provides the most recent globally gridded representation of agricultural production around 2010 (Yu et al., 2020). This dataset has been widely used to characterize the spatial distribution of crop systems and irrigation practices at the global scale.

Information on crop planting and harvest dates was obtained from the global cropping calendar developed by the Agricultural Model Intercomparison and Improvement Project (AgMIP) (Elliott et al., 2015; https://doi.org/10.5281/zenodo.3773827), which provides standardized phenological timing for major crop types. In addition to crop-specific inputs, land surface characteristics required by the model, including land cover, land use, and soil type, were taken from the WRF land surface dataset available at www2.mmm.ucar.edu.

2.3.3 Observation data

The observed data utilized in this study were obtained from the Chinese Ecosystem Research Network (CERN) through their publication on the website http://www.nesdc.org.cn. These datasets encompassed important variables such as the Leaf Area Index (LAI) and crop yield for various crops, as presented in Table 1. The purpose of utilizing these datasets was to assess and evaluate the performance of the model simulations, particularly during the parameter optimization process, which is further described in Section 2.5.

Table 1 Observation information collected from nine ecological stations.

Stations	Crops	Variable	Period	Sampling area (Crop 1/Crop 2)	Sampling number for each quadrat

https://doi.org/10.5194/egusphere-2026-2969
Preprint. Discussion started: 7 September 2026

Fengqiu (FQ)	Maize/Winter wheat	LAI,Yield	2004-2008	6-Quadrat number (10m×10m-Quadrat area)/6(10m×10m)	5(Maize)/20(Winter wheat)
Yucheng (YC)	Maize/Winter wheat	LAI,Yield	2004-2008	4(10m×10m)/4(10m×10m)	
Luancheng (LC)	Maize/Winter wheat	LAI,Yield	2004-2008	6(10m×10m)/6(10m×10m)	
Hailun (HL)	Maize/Soybean	LAI,Yield	2004-2008	6(5m×5m)/6(5m×5m)	6(Maize)/6(Soybean)
Shenyang (SY)	Maize/Soybean	LAI,Yield	2004-2008	8(6m×4m)/8(6m×4m)	
Yanting (YanT)	Rice	LAI,Yield	2004-2008	6(5m×5m)/6(5m×5m)	6(Rice)
Changshu (CS)	Rice	LAI,Yield	2004-2008	6(5m×10m)/6(5m×10m)	
Taoyuan (TY)	Early Rice	LAI,Yield	2004-2008	6(5m×5m)/6(5m×5m)	6(Early Rice)
Yingtan (YingT)	Early Rice	LAI,Yield	2004-2008	6(10m×10m)/6(10m×10m)	

2.4 Parameter optimization

In this study, we proposed a parameter optimization method based on the Morris and Sobol methods for parameter sensitivity analysis (Fig. 2). Firstly, the Morris method was employed to screen and quantify the sensitivity of parameters related to crop growth in the model (Morris, 1991; Section 2.4.2). Secondly, the Sobol' method was used to further analyze parameter sensitivity (Saltelli et al., 2000; Section 2.4.3). Next, the model simulation results from the Morris and Sobol analysis were screened using threshold values set by φ_y (φ_y<100g m^{-2}) (equation 19) and φ_l (φ_l<2) (equation 20). Parameter groups (M_a) that satisfied both conditions were selected.

https://doi.org/10.5194/egusphere-2026-2969
Preprint. Discussion started: 7 September 2026

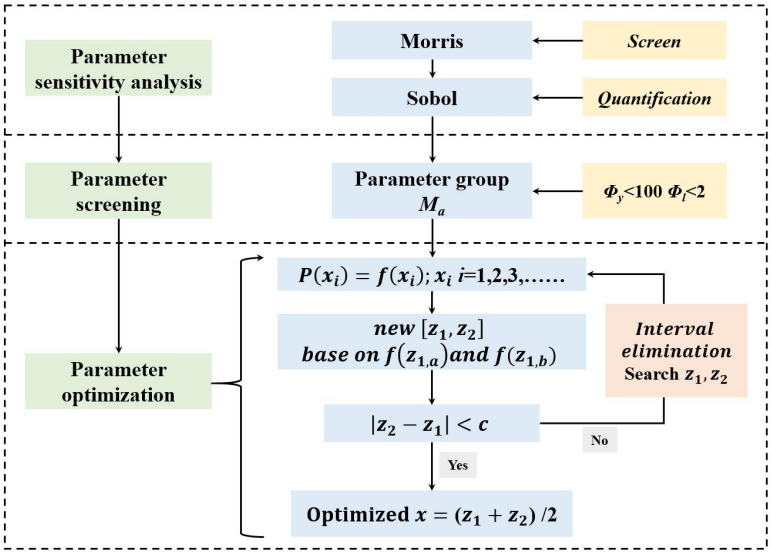

Fig.2 The flow chart of Parameter optimization.

2.4.1 The Morris method

The Morris method is a widely adopted screening technique for sensitivity analysis in computational models (Morris, 1991). Rather than relying on a fully variance-based framework, it provides a global view of parameter sensitivity by aggregating local effects-essentially first-order responses-across the parameter space (Razavi and Gupta, 2015).

For a given parameter x_i, sensitivity is quantified using the elementary effect (d_i), which measures the change in model output caused by a small perturbation in that parameter while keeping others fixed. The elementary effect is defined as:

$$d_i = \frac{y(X + \Delta_i e_i) - y(X)}{\Delta_i} \tag{10}$$

Where $X = (x_1, \ldots, x_n)$ denotes the n-dimensional parameter vector, $y(X)$ is the model output, e_i is a unit vector in the direction of parameter x_i, Δ_i is a predefined step size equal to a multiple of $1/(p-1)$, and p represents the number of discretized levels (quantiles) used to sample the parameter space.

The Morris method evaluates multiple points in the parameter hyperspace and computes summary statistics of the resulting elementary effects. Specifically, the mean value (μ) reflects the

https://doi.org/10.5194/egusphere-2026-2969
Preprint. Discussion started: 7 September 2026

overall influence of a parameter, while the standard deviation (σ) captures the presence of nonlinear effects or interactions with other parameters. To avoid cancellation effects caused by non-monotonic model behavior, we follow the recommendation of Campolongo et al. (2007) and use the mean of the absolute elementary effects (μ^*) as the primary sensitivity metric.

Both μ^* and σ are calculated across multiple sampling trajectories, which together indicate how thoroughly the parameter space has been explored. Larger μ^* values imply a stronger contribution of a parameter to model output variability, while larger σ values suggest pronounced nonlinear responses or parameter interactions (Lu et al., 2021).

2.4.2 The Sobol' method

Based on the results of the Morris screening analysis, a subset of influential parameters was selected for further investigation using the Sobol' sensitivity analysis. Parameters with a mean absolute elementary effect (μ^*) greater than 25 g m^{-2} under different conditions were considered sufficiently influential to warrant inclusion in the Sobol' analysis.

The Sobol' method is a variance-based global sensitivity analysis technique that decomposes the total variance of model output into contributions from individual input factors and their interactions (Sobol', 1990). Using an analysis of variance (ANOVA)-like framework, this method quantifies both the main effects of individual parameters and higher-order interaction effects, making it well suited for models with nonlinear responses and strong parameter interactions (Saltelli et al., 2000).

For a model with m input parameters, the total output variance $V(Y)$ can be expressed as:

$$V(Y) = \sum_{i=1}^{m} V_i + \sum_{1\le i<j\le m} V_{ij} + \cdots + V_{1,2,\ldots,m} \quad (11)$$

Here, $V_i = V[E(Y|x_i)]$ represents the variance contribution from the main effect of parameter x_i, V_{ij} represents denotes the contribution from the interaction between parameters x_i and x_j, and higher-order terms describe interactions among multiple parameters. Unlike classical ANOVA, this decomposition attributes output variability to uncertainty in the input parameters and naturally accounts for irregular and nonlinear model behavior (Monod et al., 2006)

Sensitivity indices are then derived by normalizing these variance components with respect to the total variance:

https://doi.org/10.5194/egusphere-2026-2969
Preprint. Discussion started: 7 September 2026

$$S_i = \frac{V_i}{V(Y)} \quad (12)$$

$$ST_i = \frac{V(Y) - V_{-i}}{V(Y)} \quad (13)$$

where V_{-i} is the sum of all variance components that do not involve parameter i. The first-order sensitivity index S_i measures the direct contribution of x_i to output variance, while the total sensitivity index ST_i captures the overall influence of x_i (Saltelli et al., 2000), including both its main effect and all interaction effects with other parameters.

Both S_i and ST_i range from 0 to 1. Small values indicate negligible influence on the model output, whereas values approaching 1 indicate strong control. The difference between S_i and ST_i reflects the importance of interaction effects: if S_i and ST_i are similar, the effect of parameter x_i is largely independent of other parameters, suggesting an approximately additive response. Following Vanuytrecht et al. (2014), a threshold of STi = 0.15 was adopted in this study to distinguish influential parameters from non-influential ones.

2.4.3 Optimization method

Based on the ranking of parameter sensitivity results, we constructed a function between the parameter (x_i) and the frequency ($P(x_i)$) of parameter occurrence. The function is established starting from the parameter with the greatest influence:

$$P(x_i) = f(x_i) \quad (14)$$

Here, x represents the parameter values in M_a, and i = 1, 2, 3, ... represents the order of parameter sensitivity. In this study, all $P(x_i) = f(x_i)$ functions were unimodal. The unidimensional optimization method was employed as the simplest and fundamental approach in optimization design. The unidimensional search method follows a fundamental idea of first establishing the search interval and then progressively narrowing it down through interval elimination principles to obtain an approximate solution (Nocedal & Wright., 1999). In order to determine the optimal solution by identifying the maximum frequency, we employ the golden section approach, which is suitable for finding the maximum value of any unimodal function within a predefined interval and optimizing the solution within that interval (Press, 2007). The specific methods are outlined as follows:

https://doi.org/10.5194/egusphere-2026-2969
Preprint. Discussion started: 7 September 2026

(1) Set the initial search interval [z_1, z_2] and convergence accuracy (c, set according to different parameter types). The initial values of z_1 and z_2 in this study are respectively the maximum and minimum values of the selected parameter x_i ($x_{i,min}$, $x_{i,max}$);

(2) $z_{1,a}$ and $z_{1,b}$ are calculated according to the golden section method, and the golden ratio λ is 0.618;

$$z_{1,a} = z_1 + (1-\lambda) \times (z_2 - z_1) \tag{15}$$

$$z_{1,b} = z_1 + \lambda \times (z_2 - z_1) \tag{16}$$

(3) The calculation of $f(z_{1,a})$ and $f(z_{1,b})$ based on the formula (17);

(4) According to the principle of interval elimination method, the search interval is shortened. The interval [$z_{1,a}$, $z_{1,b}$] is obtained from step 2. $f(z_{1,a})$ and $f(z_{1,b})$ have the following three cases:

$$\begin{cases} f(z_{1,a}) < f(z_{1,b}), & x_i \text{ of } P_{max}(x) \text{ in } [z_{1,b}, z_2] \\ f(z_{1,a}) > f(z_{1,b}), & x_i \text{ of } P_{max}(x) \text{ in } [z_1, z_{1,b}] \\ f(z_{1,a}) = f(z_{1,b}), & x_i \text{ of } P_{max}(x) \text{ in } [z_{1,a}, z_{1,b}] \end{cases} \tag{17}$$

where $P_{max}(x)$ is the maximum value of $P(x_i)$ in equation (13). The new search interval ($[z_1, z_2]$) is obtained by elimination method.

(5) Check whether $P(x_i)$ in the interval $[z_{1,a}, z_{1,b}]$ meets the convergence precision; if not, return to step 2; if so, take the average value of $z_{1,a}$ and $z_{1,b}$ as the approximate solution of the maximum value of $P(x_i)$.

2.4.4 Objective function

The optimization process in this study aimed to assess the agreement between observed and simulated values by minimizing an objective function. Gupta et al. (1998) proposed several objective functions suitable for parameter optimization. In this study, we employed the mean absolute error (MAE) as the objective function. Considering that different parameter values can yield similar effects, multiple objective variables, including crop yield and Leaf Area Index (LAI) at various growth stages, were considered. The objective function was formulated as follows:

$$MAE = \frac{1}{n} \cdot \sum_{t=1}^{n} |O_i - S_i| \tag{18}$$

$$\varphi_y = \frac{1}{n} \sum_{i=1}^{n} |O_{i,y} - S_{i,y}| \tag{19}$$

$$\varphi_l = \frac{1}{n} \cdot \sum_{i=1}^{n} \left(\frac{1}{m} \sum_{j=1}^{m} W_i |O_{i,l} - S_{i,l}| \right) \tag{20}$$

https://doi.org/10.5194/egusphere-2026-2969
Preprint. Discussion started: 7 September 2026

Here, φ_y represents the objective function for crop yield, φ_l represents the objective function for LAI, and n denotes the number of observed and simulated values for crop yield and LAI. O and S represent the observed and simulated values, respectively. Additionally, m corresponds to the number of crop growth periods, which is equal to 4 based on Table 2. The weighting coefficients for different growth stages, denoted as W_i, were set to 1/4 in this particular study.

Table 2 Information about the growth stage of the four crops.

Crops	Growth stages
Maize	Seedling, Elongation, Tasseling, Maturation
Rice	Tillering, Elongation, Heading, Maturation
Soybean	Seedling, Branching, Flowering, Maturation
Winter wheat	Resume growth, Elongation, Heading, Maturation

2.5 Model set-up and evaluation

In this study, 14 combinations of four crops and nine sites were considered, as detailed in Table 2, with each combination representing a distinct growing season. Model simulations covered the period from 2004 to 2008, with the 2005 data specifically used for parameter optimization across these combinations, and the data from 2004 to 2008 employed for model evaluation. To ensure the stability of initial conditions, a spin-up period from 2000 to 2003 was simulated individually prior to the start of each growing season. All simulations were conducted under irrigation-fed conditions, without accounting for water stress. The Noah-MP model encompasses various land-surface states and processes, which are listed in Table S2. Since the focus of this study is on the sensitivity of parameters related to dynamic crop growth (yield and LAI) in the Noah-MP-Crop model, the default configuration for the physical processes in the model was adopted (Table S2).

Sensitivity analysis (SA) was performed for each experimental site, with crop yield and leaf area index (LAI) as the target outputs. The Morris method was first used to identify influential parameters, using thresholds of μ^* greater than 25 g m^{-2} for crop yield and 1 for LAI. The crop yield threshold was based on Vanuytrecht et al. (2014), while the LAI threshold was determined through expert knowledge of the study area. In the Morris SA, we sampled 10 elementary effects per factor (r = 10) and considered 56 input factors (k = 56), resulting in 570 total model input sets (r(k+1) = 570) (Morris, 1991). Given the 14 crop-site combinations, this led to a total of 7,980

https://doi.org/10.5194/egusphere-2026-2969
Preprint. Discussion started: 7 September 2026

model runs (14 × 570).

After identifying the influential parameters through the Morris method, we applied the Sobol' method to further analyze these parameters. For the Sobol' analysis, we used only the remaining input factors, excluding those deemed insensitive in the Morris analysis. The number of model input sets for Sobol' analysis was determined by the formula $n(m + 2)$, where n was set to 100 or more, and m is the number of remaining parameters (Saltelli et al., 2000). In this study, 500 trajectories were used for each Sobol' sensitivity analysis, resulting in 10,500 to 15,000 model runs per site-crop combination.

Model performance was evaluated using a set of complementary statistical metrics designed to capture different aspects of simulation accuracy. Specifically, we employed the root mean square error (RMSE) following Willmott (1982), the coefficient of determination (R^2) based on the formulation of Nagelkerke (1991), and the mean absolute error (MAE). Together, these indicators were used to quantify the agreement between simulated and observed values and to provide a balanced assessment of overall model performance.

$$RMSE = \sqrt{\frac{1}{m}\sum_{i=1}^{m}(S_i - O_i)^2} \quad (21)$$

$$R^2 = 1 - \frac{\sum_{i=1}^{m}(O_i - S_i)^2}{\sum_{i=1}^{m}(O_i - \bar{O})^2} \quad (22)$$

where S_i is the simulations of model, O_i is the observations and $\bar{O}$ is the average values of the observations.

The key aspect of the parameter optimization method in this study lies in leveraging the convergence accuracy (c) to refine the initial search interval [z_1, z_2] iteratively, ultimately producing the optimal parameter range [$z_{1,a}$, $z_{1,b}$]. Consequently, in the discussion section, we also evaluated the impact of incorporating the convergence factor to demonstrate the effectiveness and robustness of our proposed method (Fig. 9,10).

https://doi.org/10.5194/egusphere-2026-2969
Preprint. Discussion started: 7 September 2026

3 Results

3.1 Sensitivity of crop growth to model parameters

3.1.1 Parameter sensitivity patterns revealed by Morris screening

The Morris screening analysis was applied to explore how crop leaf area index (LAI) and yield respond to variations in model parameters across different crops and growth stages. Fig. 3 and Fig. 4 present the normalized mean elementary effects (μ^*) for maize, rice, soybean, and winter wheat, with error bars illustrating the variability among different site-crop combinations.

For LAI (Fig. 3), a small group of parameters stands out for their consistently strong influence throughout the growing season. In particular, parameters associated with CO_2 assimilation (VCMX25, QE25, and LFMR25) dominate LAI sensitivity across all four crops. Among these, LFMR25 becomes increasingly influential toward the later growth stages, highlighting the growing importance of maintenance respiration as crops approach maturity. The effect of QE25 on winter wheat LAI is noticeably weaker than for the other crops, which is likely linked to the lower incoming solar radiation during the winter wheat growing season.

Beyond these broadly influential parameters, several others exhibit clear stage-dependent behavior. During the seedling stage, LAI variability is strongly affected by soil moisture-related parameters (SMCREF and SMCWLT) as well as the crop structural parameter BIO2LAI. As crops transition into the rapid vegetative growth phase, structural parameters (most notably BIO2LAI and LFPT_PGS3) emerge as the dominant controls on LAI ($N\mu^* > 0.5$), while the influence of soil-related parameters drops sharply ($N\mu^* < 0.1$). This shift is consistent with the model's irrigation configuration, which reduces the sensitivity of crop growth to soil moisture under non–water-stressed conditions.

During the reproductive and maturity stages, the importance of structural parameters gradually declines, and phenological parameters related to growing degree days (GDDS3 and GDDS4) become the primary drivers of LAI variability ($N\mu^* > 0.5$). This pattern reflects their role in controlling the length of vegetative and reproductive phases. Winter wheat shows a somewhat different response, with the base temperature for growing degree days (GDDTBASE) exerting a

https://doi.org/10.5194/egusphere-2026-2969
Preprint. Discussion started: 7 September 2026

stronger influence on LAI during the late growth stages than is observed for the other crops.

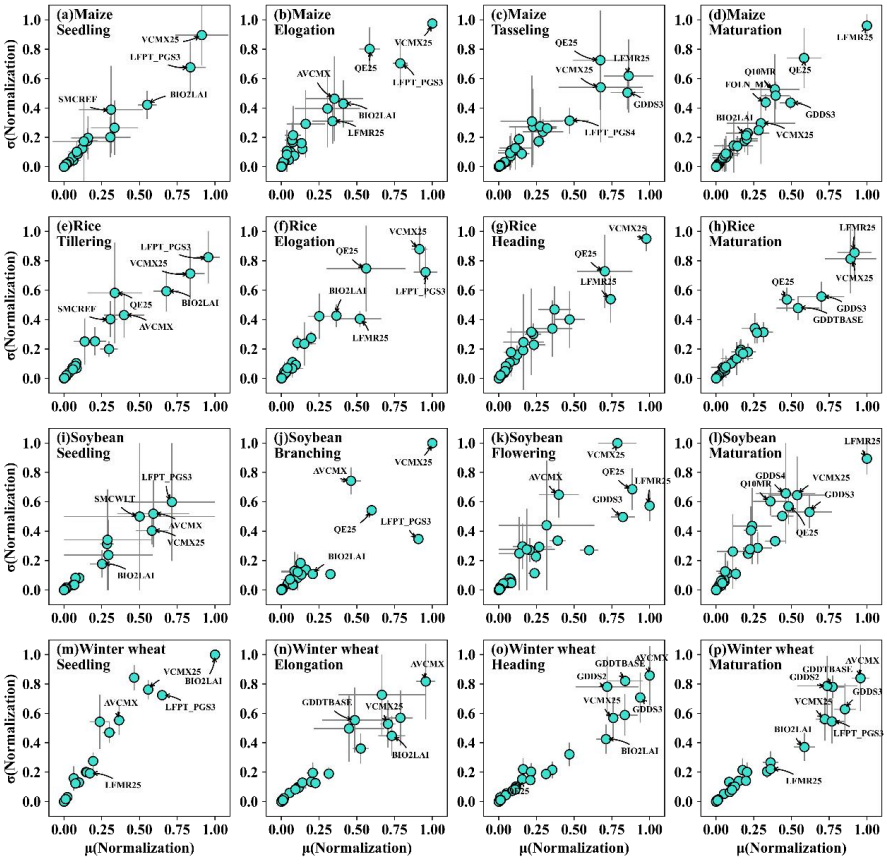

Fig. 3. The mean elementary effect of normalization ($N\mu^*$) on crop leaf area index (LAI) during different growth periods and the corresponding standard deviation of normalization ($N\sigma$) were derived from the Morris analysis for various crops. The error bars indicate standard deviation of the metrics among the site-crop combinations.

The Morris sensitivity results for crop yield (Fig. 4) reveal both clear overlaps with, and notable differences from, the patterns observed for LAI. Similar to the LAI results, parameters related to CO_2 assimilation (VCMX25, QE25, and LFMR25) show consistently strong influences on simulated yield ($N\mu^* > 0.5$), underscoring the central role of photosynthetic capacity in determining crop productivity.

Parameters associated with canopy structure and development, such as LFPT_PGS3-4 and BIO2LAI, also contribute substantially to yield variability, particularly during the rapid vegetative

https://doi.org/10.5194/egusphere-2026-2969
Preprint. Discussion started: 7 September 2026

461 growth stages. The close correspondence between LAI and yield sensitivities during this phase
462 suggests that canopy development at this stage is a key determinant of final yield. In other words,
463 what happens to the canopy early on largely sets the stage for how much grain the crop can
464 eventually produce.

465 At the same time, yield sensitivity is not entirely explained by LAI-related processes. Several
466 parameters exert a strong influence on yield while having little or no effect on LAI. A clear
467 example is GRAINPT_PGS5, which emerges as an important yield-related parameter but shows
468 negligible sensitivity for LAI, reflecting its direct role in grain formation rather than canopy
469 growth. Differences in sensitivity magnitude for parameters such as FOLN_MX further highlight
470 that parameter importance can vary depending on which model output is being considered.

471 Using a μ^* threshold of 25 g m^{-2} to identify influential parameters, between 19 and 28
472 parameters are classified as influential for yield across the four crops. Among these, a core set of
473 parameters (VCMX25, QE25, AVCMX, LFMR25, LFPT_PGS3-4, BIO2LAI, and
474 GRAINPT_PGS5) consistently shows non-negligible effects for all crops, indicating their broad
475 importance in controlling yield simulations within the Noah-MP-Crop model.

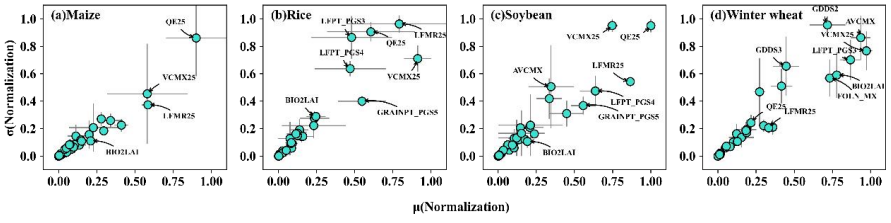

476
477 Fig.4 Mean elementary effect of normalization ($N\mu^*$) on crop yield and its standard deviation of
478 normalization ($N\sigma$) for different crops from the Morris analysis.

479 3.1.2 Quantitative parameter sensitivity and interaction effects

480 To further quantify parameter importance and the role of parameter interactions, Sobol'
481 sensitivity indices were calculated for the subset of parameters identified as influential by the
482 Morris screening. Both first-order (S_i) and total (ST_i) sensitivity indices were used to evaluate how
483 individual parameters and their interactions contribute to variations in crop leaf area index (LAI)
484 and yield.

https://doi.org/10.5194/egusphere-2026-2969
Preprint. Discussion started: 7 September 2026

For LAI, the Sobol' results for maize (Fig. 5a-d) largely mirror the patterns revealed by the Morris analysis. Parameters related to photosynthesis and canopy structure dominate LAI variability during the early growth stages, while parameters associated with leaf respiration become increasingly important as the crop develops toward maturity. The strong consistency in parameter ranking between the two methods lends confidence to the Morris screening results. At the same time, noticeable differences between STi and Si indicate that parameter interactions play a non-negligible role in shaping LAI dynamics. During the rapid vegetative growth stage, LAI variability is mainly driven by first-order effects, whereas interaction effects become more prominent during the seedling stage and again toward the end of the growing season.

Rice shows a broadly similar sensitivity pattern (Fig. 5e-h), although some crop-specific features stand out. In particular, the structural parameter LFPT_PGS3 exerts a dominant influence during the late growth stage, explaining more than 50% of the total LAI variance. For rice, differences among sites are expressed primarily through first-order sensitivity indices rather than total indices, suggesting that the overall strength of parameter interactions remains relatively stable under radiation-controlled growing conditions.

In soybean (Fig. 5i-l), parameter sensitivity peaks during the rapid vegetative growth stage, while interaction effects become more important during both early establishment and late development. Winter wheat exhibits a distinct response compared to the other crops (Fig. 5m-p). In this case, the phenological parameter GDDTBASE plays a more prominent role, accounting for approximately 20% of LAI variance during the late growth stage.

https://doi.org/10.5194/egusphere-2026-2969
Preprint. Discussion started: 7 September 2026

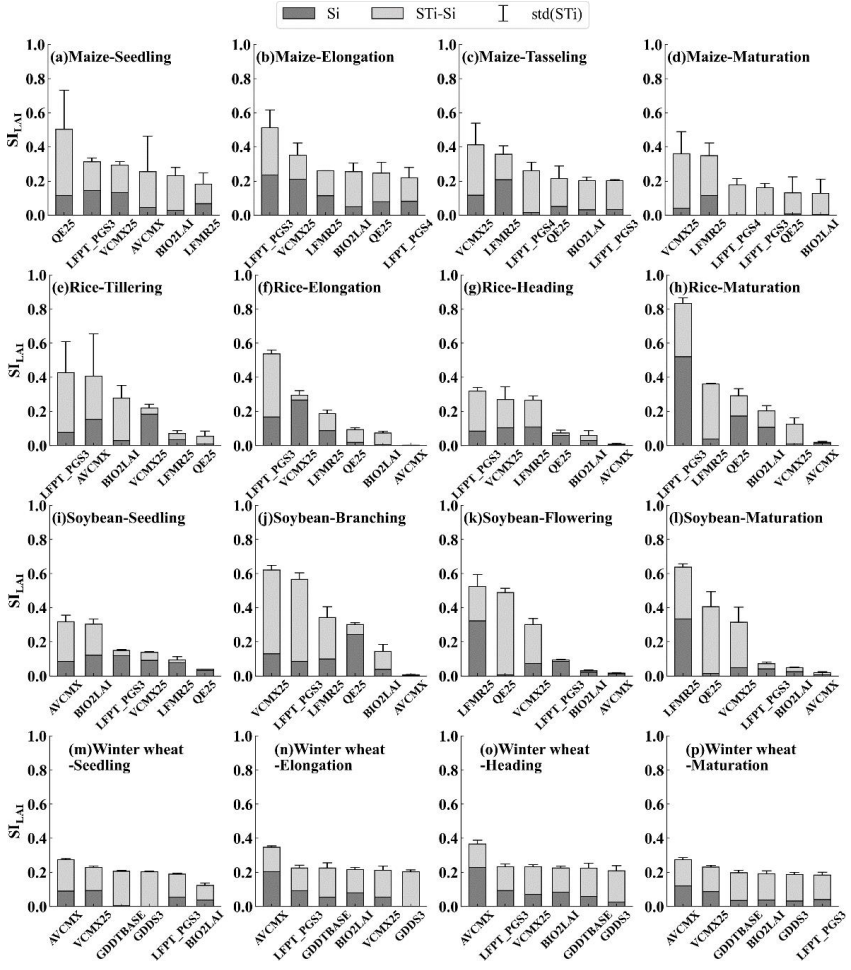

Fig.5 The sensitivity indices (SI_{LAI}) for crops LAI at different growth stages using the Sobol method. S_i indicates the first-order sensitivity, ST_i–S_i represents parameter interactions. The error bars indicate standard deviation of the metrics among the site-crop combinations. The parameters are ranked in descending order of ST_i, and only the 6 most influential parameters are plotted.

The Sobol' sensitivity analysis for crop yield (Fig. 6) reveals both shared patterns and clear crop-specific differences. For maize, rice, and soybean (Fig. 6a-c), yield variability is largely controlled by parameters related to CO_2 assimilation, most notably VCMX25, QE25, and LFMR25. In these crops, parameter interactions make a substantial contribution to yield sensitivity, accounting for roughly 30% of the difference between total and first-order sensitivity indices (ST_i - S_i). Among the assimilation-related parameters, LFMR25 stands out as particularly important for

https://doi.org/10.5194/egusphere-2026-2969
Preprint. Discussion started: 7 September 2026

soybean, where it alone explains more than 20% of the total yield variance.

Winter wheat shows a different response. Although the ranking of influential parameters is broadly consistent with the results of the Morris screening, interaction effects play a much smaller role in determining yield variability. Instead, total sensitivity is dominated by first-order effects, indicating that individual parameter contributions outweigh interactions. This pattern is likely related to the narrower parameter ranges prescribed for winter wheat, which constrain the extent to which parameter interactions can influence yield simulations.

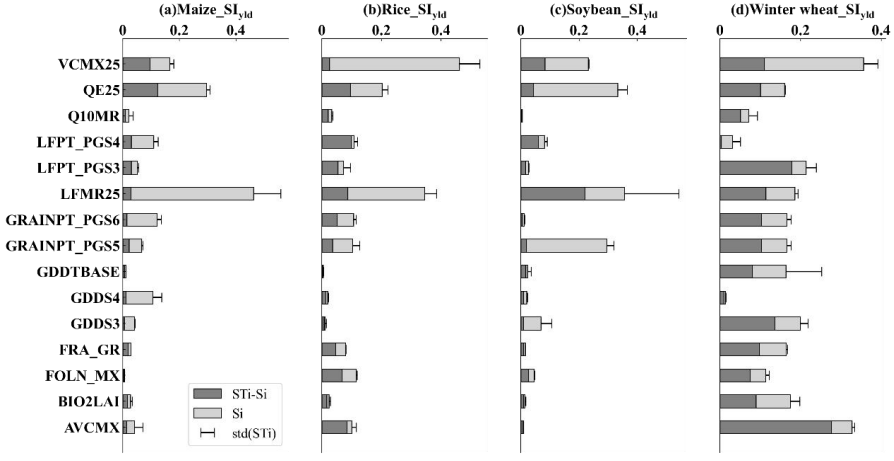

Fig.6 The sensitivity indices for different crops yield (SI_{yld}) using the Sobol method. The parameters are ranked in descending order of *Si*, and only the 15 most influential parameters are plotted.

3.1.3 Sensitivity-guided parameter optimization and optimized parameter ranges

Building on the sensitivity results from the Morris and Sobol ' analyses, the influential parameters were further refined using a sensitivity-guided optimization strategy. The optimized parameter sets for different site-crop combinations are summarized in Table 3 and Tables S3-S5. Across all crops, parameters associated with CO_2 assimilation, canopy structure, and phenological development consistently emerged as the primary targets for optimization, highlighting their central role in controlling crop growth dynamics.

https://doi.org/10.5194/egusphere-2026-2969
Preprint. Discussion started: 7 September 2026

Among the photosynthesis-related parameters, both VCMX25 and QE25 show clear variability across crops and sites. Optimized VCMX25 values range from 39.62 to 67.82 μmol m^{-2} s^{-1}. For maize, lower VCMX25 values are obtained at the SY and HL sites compared with YC, LC, and FQ, which is consistent with the cooler climatic conditions at these northern locations and the resulting constraints on Rubisco activity. In contrast, for the other crops, VCMX25 varies within a relatively narrow range across sites, reflecting the absence of strong water or nitrogen stress under the model's configuration. Optimized QE25 values fall between 0.061 and 0.085 μmol m^{-2} s^{-1} and are generally stable across crops and sites. An exception is rice at the YanT site, where lower QE25 values likely reflect weaker light conditions during the growing season.

The respiration-related parameter LFMR25 also exhibits pronounced crop-specific behavior. Optimized LFMR25 values cluster around 1.0 μmol m^{-2} s^{-1} for maize, rice, and winter wheat, whereas soybean consistently shows much lower values (< 0.5 μmol m^{-2} s^{-1}). This contrast likely reflects cooler growing-season temperatures for soybean and a reduced demand for maintenance respiration.

Structural parameters that regulate carbon allocation and canopy development display coherent patterns across crops. The leaf partitioning parameters LFPT_PGS3 and LFPT_PGS4 decrease from early to late vegetative stages, indicating a gradual shift in carbon allocation away from leaf biomass as crop development progresses. Consistent with this trend, optimized LFPT_PGS4 values are substantially lower than LFPT_PGS3 values across all sit-crop combinations. The parameter BIO2LAI, which links leaf biomass to leaf area, shows optimized values ranging from 0.017 to 0.044 m^2 g^{-1}. While site-to-site variability in BIO2LAI is relatively limited, differences among crops are more evident, reflecting contrasting growth strategies and canopy architectures.

Phenological parameters related to growing degree days, including GDD3 and GDD4, are also adjusted through the optimization process. The optimized values remain within ranges reported in previous studies, ensuring physiologically realistic representations of both early and late vegetative growth durations. Taken together, these optimized parameter ranges provide a consistent and physically plausible basis for improving crop growth simulations within the Noah-MP-Crop model.

https://doi.org/10.5194/egusphere-2026-2969
Preprint. Discussion started: 7 September 2026

Table 3 The model parameters of maize at different sites were optimized based on the results of Morris and Sobol 'sensitivity analysis.

Parameter	SY	HL	YC	LC	FQ	Unit
AVCMX	4.18	5.55	3.88	4.06	4.34	--
BIO2LAI	0.031	0.030	0.024	0.025	0.029	$m^2\ g^{-1}$
FOLN_MX	0.32	0.50	1.24	1.01	0.90	%
FRA_GR	0.13	0.10	0.06	0.07	0.04	--
GDDS3	599.63	549.74	699.44	684.43	554.37	GDD
GDDS4	1041.23	1146.11	1077.65	1033.30	1132.52	GDD
GDDTBASE	7.12	6.62	6.08	5.40	7.80	GDD
GRAINPT_PGS5	0.48	0.54	0.64	0.52	0.49	--
GRAINPT_PGS6	0.57	0.59	0.73	0.79	0.83	--
LFMR25	1.07	1.46	0.81	1.05	1.17	$\mu mol\ m^{-2}\ s^{-1}$
LFPT_PGS3	0.54	0.59	0.53	0.50	0.63	--
LFPT_PGS4	0.30	0.30	0.20	0.18	0.20	--
Q10MR	4.21	4.73	9.20	7.83	9.22	--
QE25	0.079	0.082	0.080	0.074	0.085	$\mu mol\ m^{-2}\ s^{-1}$
VCMX25	39.62	41.62	67.82	63.75	61.75	$\mu mol\ m^{-2}\ s^{-1}$

3.2 Impacts of parameter optimization on LAI and yield simulations

3.2.1 Improvement in LAI simulations across sites and crops

Model performance for leaf area index (LAI) was evaluated using multi-year mean observations at corresponding growth stages over the period 2004-2008. By averaging across years, the analysis reduces the influence of interannual variability in observational quality. Table 4 presents the LAI evaluation index (φ_l) for simulations driven by the original and optimized parameter sets, where lower φ_l values indicate better agreement with observations.

Overall, parameter optimization leads to marked improvements in LAI simulations across all crops. For winter wheat, φ_l is reduced by more than 70% at the YC, LC, and FQ sites, indicating a substantial enhancement in model performance. Rice shows consistently improved results at all sites (CS, TY, YanT, and YingT), with optimized φ_l values falling below 0.75 and reduction rates exceeding 60%. For soybean, φ_l decreases by more than 50% at both HL and SY, although it is worth noting that the original parameter set already performs relatively well at these sites ($\varphi_l < 1$). In the case of maize, parameter optimization results in an average reduction of approximately 40% in φ_l across sites.

https://doi.org/10.5194/egusphere-2026-2969
Preprint. Discussion started: 7 September 2026

582 Table 4 Comparison of crop LAI evaluation index (φ_l) between original and optimized values of
583 model parameters.

Stations	Maize		Rice		Soybean		Winter wheat	
	Original value	Optimization	Original value	Optimization	Original value	Optimization	Original value	Optimization
HL	1.50	0.81	--	--	0.86	0.42	--	--
SY	1.77	1.07	--	--	0.83	0.28	--	--
YC	2.40	1.46	--	--	--	--	2.38	0.33
LC	1.60	0.90	--	--	--	--	2.78	0.63
FQ	1.97	1.48	--	--	--	--	2.03	0.39
CS	--	--	2.15	0.62	--	--	--	--
TY	--	--	1.52	0.56	--	--	--	--
YanT	--	--	2.54	0.73	--	--	--	--
YingT	--	--	1.86	0.63	--	--	--	--

584 ### 3.2.2 Stage-dependent reductions in LAI simulation errors

585 Changes in LAI simulation accuracy across different growth stages were further evaluated
586 using mean absolute error (MAE), as shown in Fig. 7. During the seedling stage, MAE values
587 remain below 0.5 for all crops, and the differences between the original and optimized parameter
588 sets are relatively small. This indicates that LAI during the early growth stage is already
589 reasonably well represented by the model, leaving limited scope for improvement.

590 In contrast, much stronger improvements are observed during the rapid vegetative growth or
591 jointing stage. After parameter optimization, MAE values decrease by more than 40% for all crops,
592 with rice showing the largest improvement, with an MAE reduction of nearly 80%. As crops enter
593 the reproductive stage, LAI simulated with the optimized parameters closely matches observations,
594 with MAE values around 0.5 and reduction rates exceeding 50%. Improvements during this stage
595 are particularly pronounced for maize and winter wheat, both of which exhibit MAE reductions
596 greater than 80%.

597 At maturity, LAI simulations also benefit from parameter optimization. MAE values for rice,
598 soybean, and winter wheat decrease by more than 50%, indicating a clearer improvement in the
599 representation of late season canopy dynamics.

https://doi.org/10.5194/egusphere-2026-2969
Preprint. Discussion started: 7 September 2026

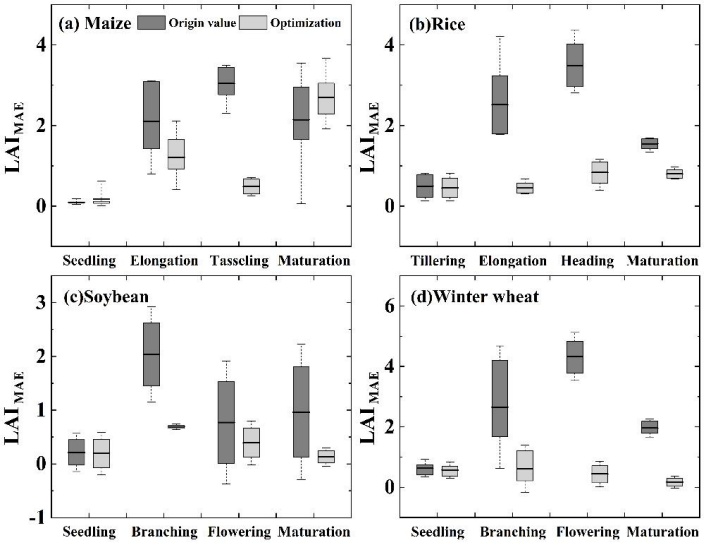

Fig.7 Comparison of MAE values for LAI of four crops at different growth stages between original and optimized values of model parameters. The boxes represent the 25th−75th percentiles, whiskers (the horizontal lines linked to boxes by the dotted line) represent the 1.5 interquartile range (IQR), and thick dashed inboxes show the mean values of all the site-crop combinations.

3.2.3 Enhanced crop yield simulations after parameter optimization

The effects of parameter optimization on crop yield simulations are shown in Fig. 8, which compares simulated and observed yields over the period 2004 to 2008. The largest improvements are observed for rice and winter wheat. When using the original parameter set, yield simulations for these two crops are strongly underestimated, and in some cases the simulated values are close to zero. After parameter optimization, agreement with observations improves substantially, with R^2 increasing to 0.88 for rice and 0.80 for winter wheat. At the same time, RMSE is reduced from 695.6 g m^{-2} to 64.0 g m^{-2} for rice and from 555.2 g m^{-2} to 83.9 g m^{-2} for winter wheat.

For maize, parameter optimization also leads to noticeable improvements. The coefficient of determination increases to 0.62, while RMSE decreases to 105.0 g m^{-2}, corresponding to improvement rates of approximately 27 percent and 77 percent, respectively. Soybean yield simulations show a different response. Although RMSE remains below 100 g m^{-2} for both the original and optimized parameter sets, the agreement with observations improves markedly, with

https://doi.org/10.5194/egusphere-2026-2969
Preprint. Discussion started: 7 September 2026

618 R^2 increasing from 0.09 to 0.64.

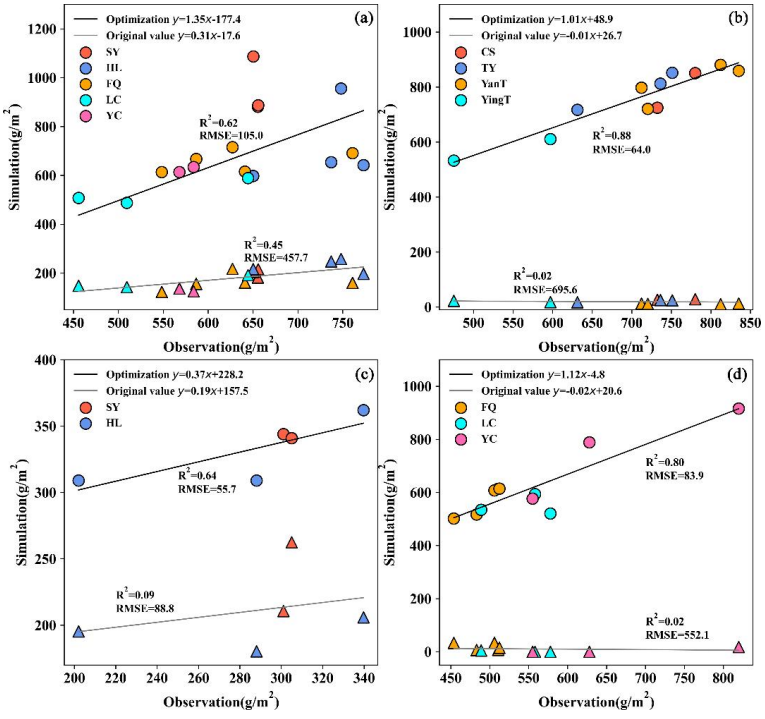

619

620 Fig.8 Comparison of RMSE and R^2 values for yield of four crops between original and optimized

621 values of model parameters. a, b, c and d represent maize, rice, soybean and winter wheat.

622 # 4 Discussion

623 ## 4.1 Key parameter controls on crop LAI and yield in Noah-MP-Crop

624 Crop growth in the Noah-MP-Crop model is represented through a series of empirical
625 formulations that describe key physiological processes, including photosynthesis, respiration,
626 carbon allocation, tissue turnover, and senescence (Liu et al., 2016). Although the model applies a
627 unified crop growth framework to different crop types, the sensitivity patterns identified in this
628 study suggest that maize, rice, and soybean are controlled by broadly similar sets of parameters,
629 with relatively limited differences among them. Winter wheat, however, shows a distinct
630 sensitivity response, which can be attributed to its longer growth period and unique phenological
631 development.

https://doi.org/10.5194/egusphere-2026-2969
Preprint. Discussion started: 7 September 2026

Across all crops, parameters regulating CO_2 assimilation consistently emerge as the dominant controls on both leaf area index (LAI) and yield. In particular, VCMX25, QE25, and LFMR25 exert strong and robust influences in both the Morris screening and Sobol' analyses. Similar sensitivity patterns have been reported in previous studies focusing on vegetation dynamics within the Noah-MP framework (Shu et al., 2022), underscoring the central role of photosynthetically assimilated carbon in driving canopy development. In Noah-MP-Crop, LAI growth is directly linked to net carbon assimilation from photosynthesis (Collatz et al., 1991), which provides a clear mechanistic explanation for the high sensitivity associated with these parameters. The importance of VCMX25 as a key determinant of photosynthetic capacity has also been widely documented in land surface and ecosystem models (Bonan et al., 2011). Comparable conclusions have been drawn from crop models based on light use efficiency or radiation driven formulations, including STICS (Brisson et al., 1998), EPIC (Williams, 1990), and CERES (Jones et al., 1986), where photosynthesis and radiation related parameters exert strong control over simulated crop growth and yield (Campos et al., 2018; Li et al., 2019).

The dominance of photosynthesis related parameters can be further understood from their physiological interpretation. VCMX25 represents the maximum carboxylation capacity of Rubisco under light saturated conditions and is fundamentally constrained by photosynthetically active radiation and enzyme kinetics (von Caemmerer and Farquhar, 1981). As a result, VCMX25 is sensitive to environmental factors such as temperature, water availability, atmospheric CO2 concentration, and soil nitrogen status, all of which influence carboxylation efficiency during leaf photosynthesis. In this study, optimized VCMX25 values for maize are lower at the SY and HL sites than at YC, LC, and FQ. This pattern is consistent with the cooler temperature conditions at SY and HL, which likely limit Rubisco activity. For the other crops, site to site variability in VCMX25 is comparatively small, reflecting the absence of strong water or nitrogen stress in the Noah-MP-Crop simulations. Optimized QE25 values fall within a relatively narrow range from 0.061 to 0.085 μmol m^{-2} s^{-1}, consistent with previous estimates of intrinsic light use efficiency (Skillman, 2008; Yin et al., 2014). The limited spatial variability in QE25 across most crops suggests that light availability plays a secondary role compared to temperature driven constraints on photosynthetic capacity.

Respiration related parameters also contribute to crop specific sensitivity patterns. LFMR25

https://doi.org/10.5194/egusphere-2026-2969
Preprint. Discussion started: 7 September 2026

represents a baseline maintenance respiration rate that is modulated by plant water status, energy availability, and air temperature (Arsenault et al., 2018). The consistently lower optimized LFMR25 values obtained for soybean compared with maize, rice, and winter wheat likely reflect cooler growing season temperatures and reduced maintenance respiration demands. This difference highlights contrasts among crops in carbon utilization efficiency.

Beyond photosynthesis and respiration, crop structural parameters play an important role in shaping canopy development and LAI dynamics. Parameters such as LFPT_PGS3 and LFPT_PGS4 regulate the allocation of assimilated carbon to leaf biomass during early and late vegetative growth stages. The optimized values indicate a progressive reduction in leaf carbon allocation as crops advance toward reproductive development. The parameter BIO2LAI governs the conversion between leaf biomass and leaf area and reflects trade offs between structural investment and light interception efficiency (Zhou et al., 2020). While optimized BIO2LAI values show relatively limited variability among sites, differences among crops are more pronounced, which is consistent with contrasting growth strategies and canopy architectures.

Crop phenology represents another important source of variability in simulated LAI and yield. Parameters controlling growing degree day requirements, including GDDS2 to GDDS4, exert a stronger influence on winter wheat than on the other crops, particularly during the late growth period. This heightened sensitivity can be explained by the longer growing season of winter wheat and its greater cumulative carbon assimilation for a given increment in growing degree days. Under these conditions, small changes in phenological timing can translate into relatively large differences in biomass accumulation. As an autumn sown crop, winter wheat requires vernalization, meaning prolonged exposure to low temperatures during early development, to achieve normal reproductive growth (Campos et al., 2018). Because vernalization processes are not explicitly represented in the Noah-MP-Crop model, phenological parameters such as GDDTBASE become especially important for controlling simulated LAI and yield in winter wheat. This limitation points to a clear direction for future model development aimed at improving the representation of winter crop phenology.

https://doi.org/10.5194/egusphere-2026-2969
Preprint. Discussion started: 7 September 2026

4.2 Implications of sensitivity-guided parameter optimization for crop modeling

Parameter optimization has long been recognized as an effective way to reduce uncertainty in land surface models, especially as these models are increasingly used in environmental assessment and climate related applications that demand higher accuracy (Shu et al., 2022; Samaniego et al., 2018). Within this broader context, the results of this study show that combining global sensitivity analysis with interval based parameter refinement can lead to substantial improvements in crop growth simulations within the Noah-MP-Crop framework.

By restricting optimization to parameters identified as influential, the sensitivity guided strategy produces clear gains in both LAI and yield simulations across all crops. Relative to simulations using the original parameter ranges, the optimized parameter intervals reduce yield RMSE by 49 to 90 percent and lower the LAI evaluation index φ_I by 39 to 81 percent, as shown in Figs. 9 and 10. These improvements are consistent with earlier studies demonstrating that targeted parameter optimization can significantly enhance model performance without incurring excessive computational costs (Sun et al., 2021). Similar advantages of interval based parameter estimation have also been reported in other modeling studies, where constraining parameter ranges helps reduce uncertainty while maintaining physical interpretability of model behavior (Waheed et al., 2020).

A key implication of this approach is that performance improvements are achieved not by expanding the parameter search space, but by narrowing it in a way that is informed by parameter sensitivity. The optimized parameter intervals consistently outperform simulations based on default parameter values, as illustrated in Figs. 7 and 8. This suggests that a substantial fraction of the uncertainty in Noah-MP-Crop simulations arises from overly broad or weakly constrained parameter ranges, rather than from limitations in model structure alone. These findings highlight the importance of sensitivity analysis as a prerequisite for efficient and robust parameter calibration in complex crop and land surface modeling systems.

https://doi.org/10.5194/egusphere-2026-2969
Preprint. Discussion started: 7 September 2026

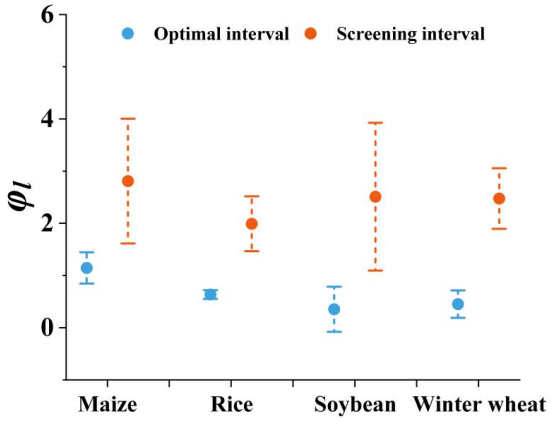

Fig.9 Comparison of φ_l values for the four crops between screening and optimal interval of model parameters.

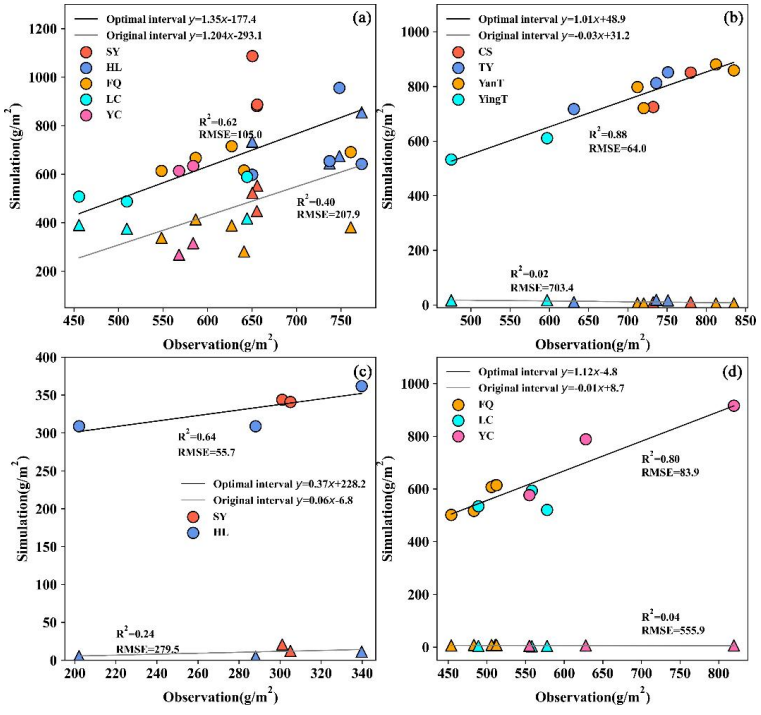

Fig.10 Comparison of RMSE and R^2 values for yield of four crops between screening and optimal interval of model parameters. a, b, c and d represent maize, rice, soybean and winter wheat.

The effectiveness of the interval based optimization also depends on how convergence criteria are defined when identifying optimal parameter ranges. In this study, convergence precision was determined using frequency based metrics derived from Sobol based parameter

https://doi.org/10.5194/egusphere-2026-2969
Preprint. Discussion started: 7 September 2026

sampling (Saltelli et al., 2000). The selected threshold captures approximately 80 percent of parameter sets that satisfy the objective function criteria φ_y<100 and φ_I<2, indicating a reasonable balance between reducing parameter uncertainty and maintaining solution robustness. The use of Latin hypercube sampling, together with sample sizes on the order of 10^4 model realizations, is consistent with existing recommendations for high dimensional parameter optimization in land surface modeling studies (Abolafia Rosenzweig et al., 2022).

Overall, these results suggest that sensitivity guided, interval based parameter optimization offers a practical and efficient pathway for improving crop representations in land surface models. Rather than adding new processes or increasing model complexity, this approach focuses on making better use of the existing model structure by identifying and constraining the parameters that exert the strongest control on simulated crop growth and yield.

5 Conclusion

This study addresses parameter uncertainty in the Noah-MP-Crop model by integrating global sensitivity analysis with sensitivity guided parameter optimization across multiple crops and agricultural sites in China. Using the Morris screening method and Sobol variance based analysis, we identify key parameters controlling crop leaf area index and yield, and clarify the relative importance of individual parameters and their interactions across growth stages. The results consistently show that parameters related to CO_2 assimilation, carbon allocation, and phenological development dominate crop growth simulations, with photosynthetic capacity, maintenance respiration, canopy structure, and growing degree day requirements exerting strong control over both LAI dynamics and final yield. While maize, rice, and soybean exhibit broadly similar sensitivity patterns, winter wheat shows distinct phenological sensitivity linked to its longer growth duration and simplified representation of winter crop processes in the model. Building on these insights, sensitivity guided parameter optimization substantially improves model performance without increasing model complexity, leading to pronounced reductions in LAI and yield errors across all crops, particularly during rapid growth and reproductive stages. Overall, this study demonstrates that combining global sensitivity analysis with targeted parameter optimization provides a practical and effective pathway for reducing parameter uncertainty and

https://doi.org/10.5194/egusphere-2026-2969
Preprint. Discussion started: 7 September 2026

improving crop growth simulations in land surface models under diverse environmental conditions.

Acknowledgements

This research was funded by the National Natural Science Foundation of China (U22A20555) and the Natural Science Foundation Project of China (42371034). The authors acknowledge the use of AI-assisted tools solely for language polishing and improving the readability of the manuscript.

Code/Data availability

No new model source code or standalone software package was developed in this study. The simulations were conducted using the Noah-MP-Crop model version 4.3. To ensure version-specific reproducibility, the exact HRLDAS/Noah-MP source-code snapshot used in this study has been permanently archived on Zenodo at https://doi.org/10.5281/zenodo.21641180 (Li et al., 2021). The current development version of the model is available from the official NCAR GitHub repository at https://github.com/NCAR/hrldas.

The optimization procedure was implemented following the methodological workflow described in Sect. 2.4.3, including parameter-sensitivity ranking, unimodal-function construction, and the golden-section search strategy. The codes and corresponding input data used for the Morris sensitivity analysis, Sobol sensitivity analysis, and parameter-optimization procedure, together with the relevant parameter files, site-based field validation data, and supporting documentation, have been publicly archived on Figshare at https://doi.org/10.6084/m9.figshare.33265260 (Li et al., 2026).

The archived materials provide the resources required to implement and reproduce the sensitivity-analysis and parameter-optimization workflows described in this study. The model configuration, parameter definitions, parameter ranges, sensitivity-analysis settings, optimization settings, and other methodological details required to understand and reproduce the analyses are

https://doi.org/10.5194/egusphere-2026-2969
Preprint. Discussion started: 7 September 2026

provided in the manuscript and the archived materials.

Author contribution

Zhonghe Li and Le Chen contributed equally to this work. Zhonghe Li and Chesheng Zhan conceived and designed the study. Zhonghe Li and Le Chen performed the model development, sensitivity analysis, parameter optimization, and result analysis. Shi Hu, Like Ning, Lanfang Wu, Hai Guo, and Qi Zhang contributed to data collection, interpretation of results, and manuscript revision. Zhonghe Li prepared the original draft. Chesheng Zhan supervised the research and revised the manuscript. All authors read and approved the final manuscript.

Competing interests

The contact author has declared that none of the authors has any competing interests.

References

Abolafia-Rosenzweig, R., He, C., McKenzie Skiles, S., Chen, F., Gochis, D., 2022. Evaluation and Optimization of Snow Albedo Scheme in Noah-MP Land Surface Model Using In Situ Spectral Observations in the Colorado Rockies. J. Adv. Model. Earth Syst. 14(10), e2022MS003141.

Araya, S., Ostendorf, B., Lyle, G., Lewis, M., 2018. CropPhenology: An R package for extracting crop phenology from time series remotely sensed vegetation index imagery. Ecol Inform, 46, 45-56.

Arsenault, K.R., Nearing, G.S., Wang,S., Yatheendradas, S., Peters-Lidard, C.D., 2018. Parameter sensitivity of the Noah-MP land surface model with dynamic vegetation. J Hydrometeorol, 19(5), 815-830.

Balderas, F., Fernandez, E., Gomez-Santillan, C., Rangel-Valdez, N., Cruz, L., 2019. An interval-based approach for evolutionary multi-objective optimization of project portfolios.

https://doi.org/10.5194/egusphere-2026-2969
Preprint. Discussion started: 7 September 2026

Int J Inf Technol Decis Mak, 18(04), 1317-1358.

Bonan, G.B., et al., 2011. Improving canopy processes in the Community Land Model version 4 (CLM4) using global flux fields empirically inferred from FLUXNET data. J. Geophys. Res, 116(G2), G02014.

Boote, K.J., Jones, J.W., Batchelor, W.D., Nafziger, E.D., Myers, O., 2003. Genetic coefficients in the CROPGRO–Soybean model: Links to field performance and genomics. Agron J, 95(1), 32-51.

Brisson, N., et al., 1998. STICS: a generic model for the simulation of crops and their water and nitrogen balances. I. Theory and parameterization applied to wheat and corn. Agronomy, 18(5-6), 311-346.

Campolongo, F., Cariboni, J., Saltelli, A., 2007. An effective screening design for sensitivity analysis of large models. Environ. Model. Softw. 22, 1509–1518.

Campos, I., et al., 2018. Remote sensing-based crop biomass with water or light-driven crop growth models in wheat commercial fields. Field Crops Res. 216, 175–188.

Collatz, G.J., Ball, J.T., Grivet, C., Berry, J.A., 1991. Physiological and environmental regulation of stomatal conductance, photosynthesis and transpiration: A model that includes a laminar boundary layer. Agric For Meteorol, 54(2-4), 107–136.

Confalonieri, R., et al., 2010. Sensitivity analysis of the rice model WARM in Europe: exploring the effects of different locations, climates and methods of analysis on model sensitivity to crop parameters. Environ Model Softw, 25(4), 479-488.

Drewniak, B., Song, J., Prell, J., Kotamarthi, V. R., Jacob, R., 2013. Modeling agriculture in the community land model. Geosci Model Dev, 6(2), 495-515.

Elliott, J., et al., 2015. The global gridded crop model intercomparison: data and modeling protocols for phase 1 (v1. 0). Geosci Model Dev, 8(2), 261-277.

Ferreyra, R.A., 2004. A faster algorithm for crop model parameterization by inverse modeling: simulated annealing with data reuse. Trans. ASAE, 47(5), 1793-1801.

Gupta, H.V., Sorooshian, S., Yapo, P.O., 1998. Toward improved calibration of hydrologic models: Multiple and noncommensurable measures of information. Water Resour. Res. 34(4), 751-763.

Hu, S., Mo, X., Lin, Z., 2014. Optimizing the photosynthetic parameter Vcmax by assimilating

https://doi.org/10.5194/egusphere-2026-2969
Preprint. Discussion started: 7 September 2026

MODIS-fPAR and MODIS-NDVI with a process-based ecosystem model. Agric For Meteorol, 198, 320-334.

Jin, X., et al., 2018. Parameter sensitivity analysis of the AquaCrop model based on extended fourier amplitude sensitivity under different agro-meteorological conditions and application. Field Crops Res. 226, 1-15.

Jones, C.A., Kiniry, J.R., Dyke, P.T., 1986. CERES-Maize: A simulation model of maize growth and development.

Levis, S., et al., 2012. Interactive crop management in the Community Earth System Model (CESM1): Seasonal influences on land–atmosphere fluxes. J. Clim, 25(14), 4839-4859.

Li, Z.H., Chen, L., Hu, S., 2026. Data and code. figshare. Dataset. https://doi.org/10.6084/m9.figshare.33265260.v4.

Li, Z.H., Chen, L., Ning, L.K., Guo, H., 2021. HRLDAS/Noah-MP unified repository source code snapshot (commit 8036b3b) (Versions 8036b3b3cbd853b810e6b3feb2becbeffdb81111) [Computer software]. Zenodo. https://doi.org/10.5281/zenodo.21641180.

Li, Z.h., Jin, X.l., Liu, H.l., Xu, X.g., Wang, J.h., 2019. Global sensitivity analysis of wheat grain yield and quality and the related process variables from the DSSAT-CERES model based on the extended Fourier Amplitude Sensitivity Test method. J. Integr. Agric. 18, 1547–1561.

He, L.H., Mo, X.G., Hu, S., Liu, S.X., 2021. Global sensitivity and uncertainty analysis of the VIP ecosystem model with an expanded soil nitrogen module for winter wheat-summer maize rotation system in the North China Plain. Pedosphere, 31(5), 822-838.

Liu, X., Chen, F., Barlage, M., Zhou, G., Niyogi, D., 2016. Noah-MP-Crop: Introducing dynamic crop growth in the Noah-MP land surface model. J. Geophys. Res. Atmos. 121(23), 13-953.

Lobell, D.B., Bala, G., Duffy, P.B., 2006. Biogeophysical impacts of cropland management changes on climate. Geophys. Res. Lett. 33(6).

Lokupitiya, E., et al., 2009. Incorporation of crop phenology in Simple Biosphere Model (SiBcrop) to improve land-atmosphere carbon exchanges from croplands. Biogeosciences, 6(6), 969-986.

Lu, Y., Chibarabada, T.P., McCabe, M.F., De Lannoy, G.J., Sheffield, J., 2021. Global sensitivity analysis of crop yield and transpiration from the FAO-AquaCrop model for dryland environments. Field Crops Res. 269, 108182.

https://doi.org/10.5194/egusphere-2026-2969
Preprint. Discussion started: 7 September 2026

865 Monod, H., Naud, C., Makowski, D., 2006. Uncertainty and sensitivity analysis for crop models.
866 In: Wallach, D., Makowski, D., Jones, J.W. (Eds.), Working With Dynamic Crop Models:
867 Evaluation, Analysis, Parameterization, and Applications. Elsevier, UK, pp. 55–100.
868 Morris, M.D., 1991. Factorial sampling plans for preliminary computational experiments.
869 Technometrics 33, 161–174.
870 Niu, G.Y., et al., 2020. Enhancing the Noah-MP ecosystem response to droughts with an explicit
871 representation of plant water storage supplied by dynamic root water uptake. JJ. Adv. Model.
872 Earth Syst. 12(11), e2020MS002062.
873 Niu, G.Y., Yang, Z.L., 2004. Effects of vegetation canopy processes on snow surface energy and
874 mass balances. J. Geophys. Res. Atmos. 109(D23).
875 Niu, G.Y., et al., 2011. The community Noah land surface model with multiparameterization
876 options (Noah-MP): 1. Model description and evaluation with local-scale measurements. J.
877 Geophys. Res. Atmos. 116(D12).
878 Nocedal, J., & Wright, S. J. (Eds.)., 1999. Numerical optimization. New York, NY: Springer New
879 York.
880 Pianosi, F., Wagener, T., 2015. A simple and efficient method for global sensitivity analysis based
881 on cumulative distribution functions. Environ Model Softw, 67, 1-11.
882 Pianosi, F., et al., 2016. Sensitivity analysis of environmental models: A systematic review with
883 practical workflow. Environ Model Softw, 79, 214-232.
884 Pitman, A.J., et al., 2009. Uncertainties in climate responses to past land cover change: First
885 results from the LUCID intercomparison study. Geophys. Res. Lett. 36(14).
886 Press, W.H., 2007. Numerical recipes 3rd edition: The art of scientific computing. Cambridge
887 university press.
888 Razavi, S., Gupta, H.V., 2015. What do we mean by sensitivity analysis? The need for
889 comprehensive characterization of “global” sensitivity in Earth and environmental systems
890 models. Water Resour. Res. 51, 3070–3092.
891 Rosolem, R., et al., 2013. Towards a comprehensive approach to parameter estimation in land
892 surface parameterization schemes. Hydrol Process, 27(14), 2075-2097.
893 Saltelli, A., Tarantola, S., Campolongo, F., 2000. Sensitivity analysis as an ingredient of modeling.
894 Stat. Sci. 15 (4), 377–395.

https://doi.org/10.5194/egusphere-2026-2969
Preprint. Discussion started: 7 September 2026

895 Samaniego, L., et al., 2018. Anthropogenic warming exacerbates European soil moisture droughts.
896 Nat Clim Change, 8(5), 421-426.
897 Shu, Z., Zhang, B., Tian, L., Zhao, X., 2022. Improving Dynamic Vegetation Modeling in
898 Noah-MP by Parameter Optimization and Data Assimilation Over China's Loess Plateau. J.
899 Geophys. Res. Atmos. 127(19), e2022JD036703.
900 Silvestro, P.C., et al., 2017. Sensitivity analysis of the Aquacrop and SAFYE crop models for the
901 assessment of water limited winter wheat yield in regional scale applications. PloS one,
902 12(11), e0187485.
903 Skillman, J.B., 2008. Quantum yield variation across the three pathways of photosynthesis: not yet
904 out of the dark. J. Exp. Bot. 59(7), 1647-1661.
905 Sobol', I.Y.M., 1990. On sensitivity estimation for nonlinear mathematical models. Mat. model. 2
906 (1), 112–118.
907 Sun, R., Duan, Q., Huo, X., 2021. Multi-Objective Adaptive Surrogate Modeling-Based
908 Optimization for Distributed Environmental Models Based on Grid Sampling. Water Resour.
909 Res. 57(11), e2020WR028740.
910 Tsarouchi, G.M., Buytaert, W., Mijic, A., 2014. Coupling a land-surface model with a crop growth
911 model to improve ET flux estimations in the Upper Ganges basin, India. Hydrol Earth Syst
912 Sci, 18(10), 4223-4238.
913 Van den Hoof, C., Hanert, E., Vidale, P.L., 2011. Simulating dynamic crop growth with an adapted
914 land surface model–JULES-SUCROS: Model development and validation. Agric For
915 Meteorol, 151(2), 137-153.
916 Vanuytrecht, E., Raes, D., Willems, P., 2014. Global sensitivity analysis of yield output from the
917 water productivity model. Environ. Modell. Softw. 51, 323–332.
918 Von Caemmerer, S.V., Farquhar, G.D., 1981. Some relationships between the biochemistry of
919 photosynthesis and the gas exchange of leaves. Planta, 153, 376-387.
920 Wagner, M.P., Slawig, T., Taravat, A., Oppelt, N., 2020. Remote sensing data assimilation in
921 dynamic crop models using particle swarm optimization. ISPRS Int. J. Geoinf, 9(2), 105.
922 Waheed, S.Q., Grigg, N.S., Ramirez, J.A., 2020. Variable infiltration-capacity model sensitivity,
923 parameter uncertainty, and data augmentation for the Diyala River Basin in Iraq. J Hydrol
924 Eng, 25(9), 04020040.

https://doi.org/10.5194/egusphere-2026-2969
Preprint. Discussion started: 7 September 2026

925 Wang, J.B., Wang, J.W., Ye, H., Liu, Y., He, H.L., 2017. An interpolated temperature and
926 precipitation dataset at 1-km grid resolution in China (2000 – 2012). China Scientific Data
927 Vol. 2, No. 1.
928 Wang, J., Li, X., Lu, L., Fang, F., 2013. Parameter sensitivity analysis of crop growth models
929 based on the extended Fourier Amplitude Sensitivity Test method. Environ Model Softw, 48,
930 171-182.
931 Williams, J.R., 1990. The erosion-productivity impact calculator (EPIC) model: a case history.
932 Philosophical Transactions of the Royal Society of London. Series B: Biological Sciences,
933 329(1255), 421-428.
934 Willmott, C.J., 1982. Some comments on the evaluation of model performance. Bull Amer Meteor
935 Soc. 63: 1309–1313.
936 Xu, T., et al., 2021. Improve the Performance of the Noah-MP-Crop Model by Jointly
937 Assimilating Soil Moisture and Vegetation Phenology Data. J. Adv. Model. Earth Syst. 13(7).
938 Xu, X., et al., 2019. Lessons learned from modeling irrigation from field to regional scales. J. Adv.
939 Model. Earth Syst. 11(8), 2428-2448.
940 Yin, X., Belay, D.W., van der Putten, P.E., Struik, P.C., 2014. Accounting for the decrease of
941 photosystem photochemical efficiency with increasing irradiance to estimate quantum yield
942 of leaf photosynthesis. Photosyn. Res. 122, 323-335.
943 Yu, L., et al., 2022. Coupling localized Noah-MP-Crop model with the WRF model improved
944 dynamic crop growth simulation across Northeast China. Comput Electron Agric, 201,
945 107323.
946 Yu, Q., et al., 2020. A cultivated planet in 2010–Part 2: The global gridded agricultural-production
947 maps. Earth Syst. Sci. Data, 12(4), 3545-3572.
948 Zhang, C., Li, X., Guo, P., Huo, Z., 2020. An improved interval-based fuzzy
949 credibility-constrained programming approach for supporting optimal irrigation water
950 management under uncertainty. Agric Water Manag, 238, 106185.
951 Zhang, Z., et al., 2020. Joint modeling of crop and irrigation in the central United States using the
952 Noah-MP land surface model. J. Adv. Model. Earth Syst. 12(7), e2020MS002159.
953 Zhou, H., et al., 2020. Environmental explanation of maize specific leaf area under varying water
954 stress regimes. Environ. Exp. Bot. 171, 103932.

https://doi.org/10.5194/egusphere-2026-2969
Preprint. Discussion started: 7 September 2026

955